19940020873

N94- 25355

MEASURING TRACK DENSITIES IN LUNAR GRAINS BY IMAGE ANALYSIS

Final Report
NASA/ASEE Summer Faculty Fellowship Program--1993
Johnson Space Center

Prepared By:	George E. Blanford, Ph.D.
Academic Rank:	Professor
University and Department:	University of Houston-Clear Lake School of Natural and Applied Sciences Houston, TX 77058

NASA/JSC

Directorate:	Space and Life Sciences
Division:	Solar System Exploration
Branch:	Planetary Sciences
JSC Colleague:	David S. McKay, Ph.D.
Date Submitted:	August 6, 1993
Contract Number:	NGT-44-001-800

ABSTRACT

We have developed techniques to use digitized scanning electron micrographs and computer image analysis programs to measure track densities in lunar soil grains. Tracks were formed by highly ionizing solar energetic particles and cosmic rays during near surface exposure on the Moon. The track densities are related to the exposure conditions (depth and time). Distributions of the number of grains as a function of their track densities can reveal the modality of soil maturation. We used a sample that had already been etched in 6 N NaOH at 118°C for 15 h to reveal tracks. We determined that back-scattered electron images taken at 50% contrast and ~49.8% brightness produced suitable high contrast images for analysis. We ascertained gray-scale thresholds of interest: 0-230 for tracks, 231 for masked regions, and 232-255 for background. We found no need to set an upper size limit for distinguishing tracks. We did use lower limits to exclude noise: 16 pixels at 15000x, 4 pixels at 10000x, 2 pixels at 6800x, and 0 pixels at 4600x. We used computer counting and measurement of area to obtain track densities. We found an excellent correlation with manual measurements for track densities below 1×10^8 cm^{-2}. For track densities between 1×10^8 cm^{-2} to 1×10^9 cm^{-2} we found that a regression formula using the percentage area covered by tracks gave good agreement with manual measurements. Finally we used these new techniques to obtain a track density distribution that gave more detail and was more rapidly obtained than using manual techniques 15 years ago.

INTRODUCTION

Solar wind, solar energetic particles, galactic cosmic rays, and meteoroid impacts hit regolith grains on the Moon, asteroids, some planets and satellites, and interplanetary dust particles producing measurable forms of "weathering.". Research has shown that these measurable effects correlate in lunar soils (McKay *et al.*, 1991). Nevertheless, the correlations are very crude because the weathering effects on the Moon are usually measured as a bulk average for a given soil. Most weathering measurements are not very useful for making quantitative predictions of exposure age or even giving a relative measure of maturity for the soil. Furthermore, regolith soils mature by at least two distinct processes: by *in situ* weathering and by mixing. Bulk average measurements cannot distinguish the maturation processes. To improve our understanding of space weathering, we should find these correlations on a grain by grain basis. During the ASEE summer program, we concentrated principally on one form of weathering, the formation of tracks in individual soil grains caused by solar energetic particles and galactic cosmic rays.

Price and Walker (1962) discovered that very ionizing radiation, such as fission fragments and cosmic rays, produces a trail of damage in dielectric materials that can be etched with a reagent to form visible tracks (cf. Fleischer *et al.*, 1975). Their discovery has led to practical applications such as Nuclepore filter paper and cosmic ray dosimeters used by astronauts. Scientific applications include fission track dating of geological samples and, the subject of our research, cosmic ray-solar energetic particle weathering effects on lunar samples. From the beginning quantitative scientific results have followed from counting tracks on micrographs and by micrographically measuring track morphological characteristics. The sophistication and ready availability of image processing software can reduce this tedious labor.

Etching lunar soil grains in a suitable reagent reveals tracks by producing pits at the track locations. We used a scanning electron microscope (SEM) to make digital images of the etched surfaces of polished grain mounts. We developed procedures to rapidly measure track densities with image processing software. We applied these techniques to determine the track density distribution at one level in a lunar core that we compared to measurements made 15 years ago using conventional techniques.

EXPERIMENTAL DETAILS

This summer project concentrated on the development of image processing techniques and not on the techniques of track etching. Consequently we used a lunar soil sample that had been prepared and etched 15 years ago. Although this sample had been returned to the lunar sample curator, it had been rerequested several years ago to show etched tracks to a Japanese film crew and was still in my advisors safe. It was a polished section of an Apollo 16 double drive tube numbered 60009, 6049. Photomicrographs of this sample were available to aid in the location of particular zones of interest. We chose to work at a position that we estimate to be 546 mm below the lunar surface. This sample had been etched for 15 hours in 6 N sodium hydroxide at 118°C. It was also already coated with a vacuum deposited layer of gold to prevent charging in the SEM.

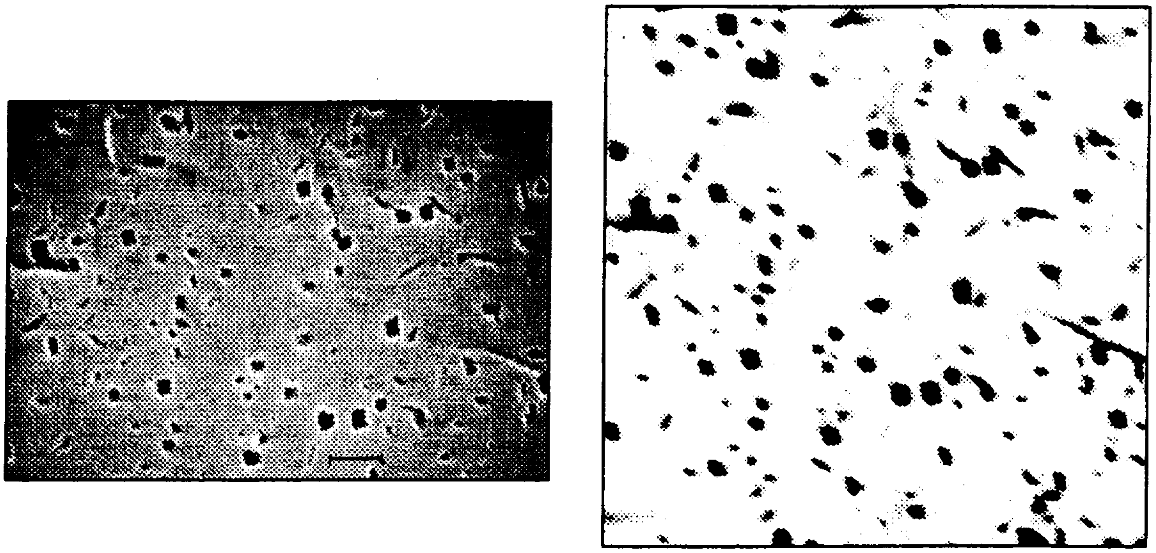

Figure 1. a) The image on the left is a secondary electron image of a lunar plagioclase grain with a track density of 1.7×10^{8} cm^{-2}. The bar is 1 μm. b) The image on the right is a digitized back-scattered electron image of the same grain.

We obtained images on an ISI SEM. The sample was oriented perpendicular to the electron beam. The same condenser lens setting and aperture were used for all images. Nevertheless, the microscope is not equipped with a Faraday cup and we could not be sure of reproducing the same beam current exactly for each microscope session. The working distance knob was set at 8 mm, the focus knobs were set at 5 turns clockwise, and the image was brought into focus initially by adjusting the sample height. This procedure assures that magnification and resolution will be consistent from one session to another. We determined magnification calibration with a stage micrometer and verified that it remained consistent within 1.5%. The SEM is capable of making conventional secondary electron images (SEI) and it is also equipped with a back-scattered electron (BSE) detector. Secondary electrons produce a gray scale micrograph that looks very much like a regular black and white photograph (Fig. 1a). If SEI were used, we felt that fairly sophisticated image processing would be necessary to use the computer to distinguish tracks from background. BSE images, however, naturally showed a high contrast between tracks and background. We purposely chose to exploit this property and took digital images that appeared to the naked eye to be almost binary with very little gray (Fig. 1b). Using the computer we could set the contrast and brightness to numerically reproducible settings. We chose a wide variety of contrast settings and adjusted brightness settings visually to reproduce a high contrast image. We could not determine any significant quantitative differences when these images were analyzed for many different contrast settings. We chose to work at a contrast setting of 50%. The brightness setting was at about 49.8%, but it had to be adjusted slightly at different sessions on the SEM, probably because the beam current was not exactly reproducible.

We produced digital images and analyzed them using an eXL computer manufactured by Oxford Instruments, formerly Link Analytical. The computer has a proprietary operating system and software. The system is designed to be used with electron microscopes and it controls energy dispersive x-ray analysis as well as digital imaging. There are a wide variety of image processing options and analytical options. I will describe only those procedures that were useful to us. Digital images were collected as a Kalman average for 90 sec. The images were 512 x 512 pixels at a 256 gray-scale (8 bit). We consistently worked at 4 different magnifications, 4600x, 6800x, 10000x, and 15000x (we also tried 2200x and 22000x, but found these magnifications to be impractical). After acquiring the image, we created a mask for the image to obscure parts of the image we did not wish to analyze such as areas off the edge of the grain, large cracks, *etc*. We could "paint" the image using this mask to some useful gray-scale level. Masking was not always necessary, but was more necessary at lower magnifications such as 4600x and 6800x. We found two analytical procedures useful. One of these, called "feature scan," actually counts the tracks. The other procedure, called "single image phase analysis," measures areas. Dividing the number of tracks by the area gives the track density.

FEATURE SCAN

The "feature scan" subset of routines is capable of doing many analytical procedures on an image. In future work we will take advantage of some of its capabilities regarding the morphology of "features," but for this work our needs were relatively simple.

A "feature" is defined in terms of connected areas (pixels) within defined limits of gray-scale. Because we took high contrast images, it was relatively simple to define these limits. The lower limit was 0 on the 256 gray-scale. By trial and error the upper limit was set to obtain track counts that were consistent with manual track counts on several standard images. The upper threshold that we finally established was 230. On images that were masked, the masked region was "painted" 231. In addition to setting thresholds, size criteria could also be used. The program counted every connected "feature" within the gray-scale thresholds, but it distinguished some as too big and others as too small. Again trial and error were used to set these size criteria. Eventually it was determined not to set maximum size criteria. The minimum size criteria were set as follows (in pixels): 16 at 15000x, 4 at 10000x, 2 at 6800x, none at 4600x. We also set the "connectivity" to 8 pixels.

With these settings established and set, we simply direct the software to "detect and measure." The image is scanned and each "feature" or track is counted. A cartoon-like image appears on the screen showing and numbering each "feature." The operator can look at this image and make a qualitative judgment about the success of the procedure. The total count is displayed on the screen as well as the counts within the categories of "too big," "too small," and just right.

SINGLE IMAGE PHASE ANALYSIS

The "single image phase analysis" subset of routines prepares a histogram of pixel number versus the image gray-scale levels and allows the user to interactively set thresholds that are color coded. The routine displays the area covered by each threshold region in pixels, in square micrometers (if you have calibrated and set the magnification at the time the image was collected), and percentage of total area. Before we established the threshold level

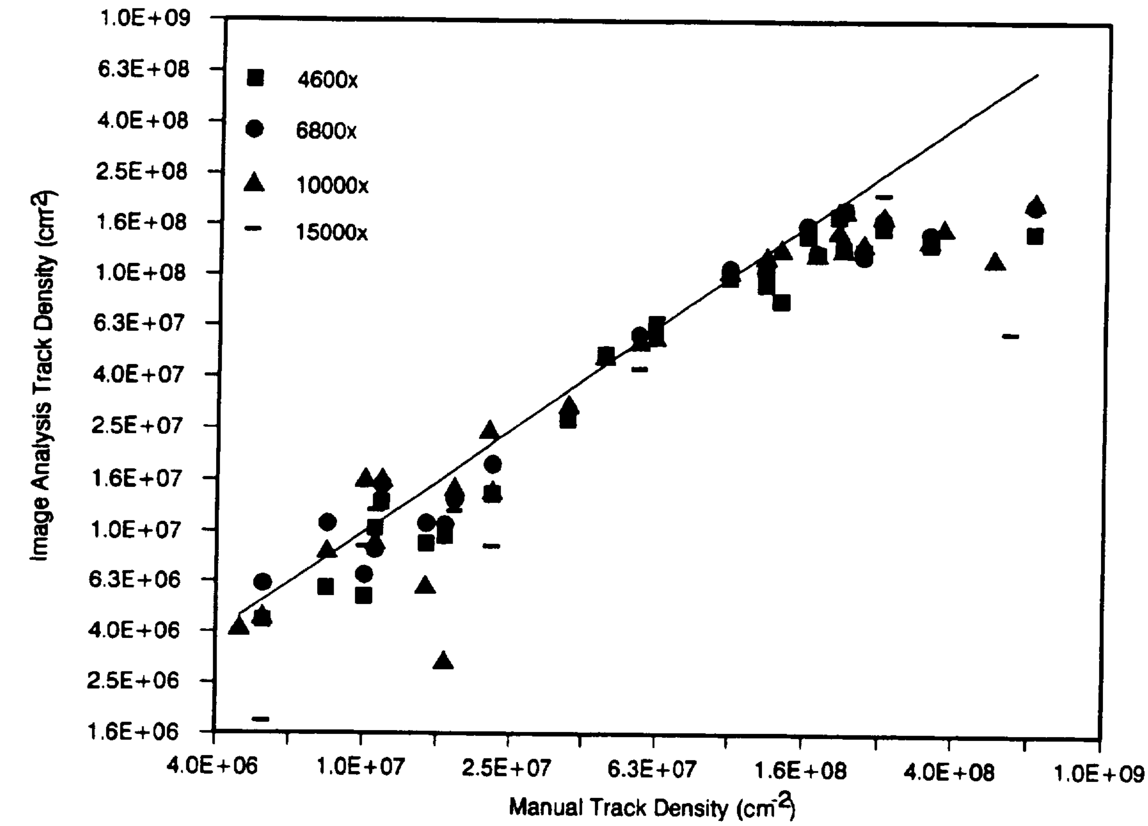

Figure 2. Graph of track densities in lunar soil grains from sample 60009, 6049 at a depth of 546 mm from the lunar surface from images taken at 4600x, 6800x, 10000x, and 15000x. The ordinate has values determined from counts using "feature scan." The abcissa has values determined by manual counting.

of 230 using "feature scan," we examined several different threshold settings on a trial and error basis. The final settings were 0-230 for tracks, 231 for the mask, and 232-255 for background. Using this routine, we could determine the total area of the image, the area of the mask, and the percentage area covered by tracks.

RESULTS

Figure 2 shows a correlation diagram of track density measurements using image analysis with conventional measurements from a photomicrograph. The correlation is excellent for track densities below 1×10^8 cm^{-2}. Furthermore, the correlation is not sensitive to the magnification used within the range tested (but there is better statistical accuracy for lower track density grains when measured at lower magnifications). However, above track densities of 1×10^8 cm^{-2} the image analysis technique shows saturation. It is not hard to understand why this is true. In Fig. 3a and b we show images for a point on the far right side of Fig. 2. The human counter can distinguish overlapping tracks to some extent (although this image is approaching the limit for human counting too). The software however lumps many tracks into single "features" on the digital image and the computer

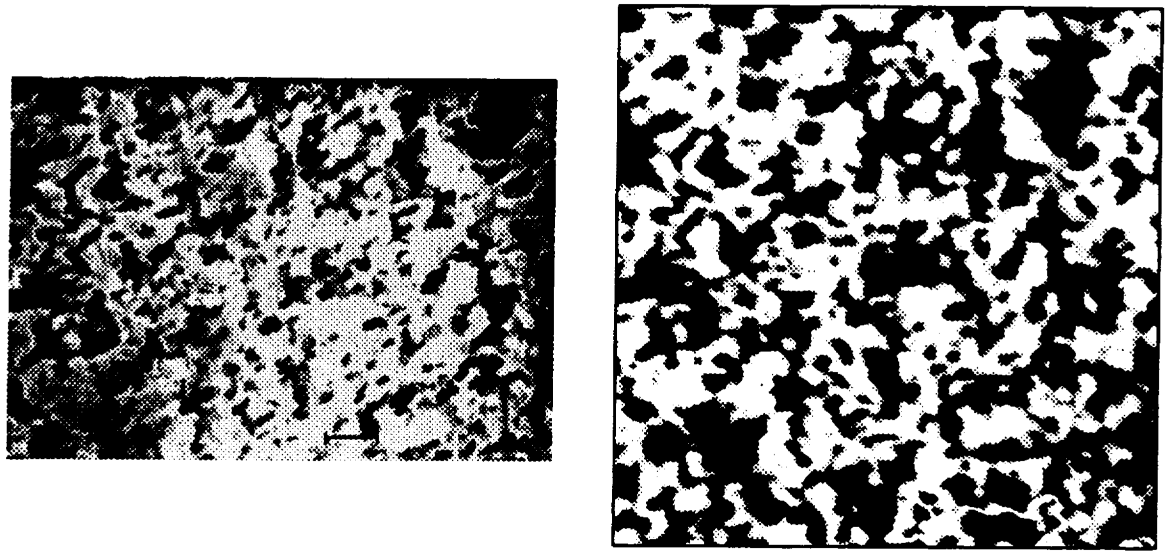

Figure 3. a) The image on the left is a secondary electron image of a lunar plagioclase grain with a track density of $5.6x10^8$ cm^{-2}. The bar is 1 μm. b) The image on the right is a digitized back scattered image of the same grain. Tracks are severly overlapped.

under counts. My advisor suggested a way around this problem. The area covered by the tracks should be proportional to the number of tracks. In Fig. 4 we show a graph of track density versus the percentage area covered by tracks for images taken at 10000x that we get from the "single image phase analysis" routines. The linear regression line has a correlation coefficient r=.98. Consequently, we can use this regression line to determine track densities from $1x10^8$ cm^{-2} to $1x10^9$ cm^{-2}. Even this method is likely to fail at higher track densities. Figure 5 shows the 10000x data from Fig. 2 together with corrected points using the regression formula. The rectangles surrounding each point represent one standard deviation statistical uncertainty.

Although most of the time allotted to this project was spent in establishing the correct conditions for measuring track densities using image analysis software, we wanted to do one practical measurement using our techniques. Because we were using a lunar core sample, we could measure a distribution of the number of grains as a function of track density. Blanford *et al.* (1979) (or McKay *et al.*, 1991) have discussed the relationship of the track density distribution to the modality of soil maturation. They have also measured the track density distribution of the 60009 core at the depth of 546 mm. Using the faster methods of computer image analysis we have remeasured this distribution. We collected 48% of the data for this distribution in only two microscope sessions. We compare the two distributions in Fig. 6. Clearly the distribution using 100 grains that was obtained from computer image techniques shows more detail; it is clearly a bimodal distribution that indicates that the soil at 546 mm in the 60009 core is a mixed soil (Blanford *et al.*, 1979). The disturbing difference between the two distributions is the overall shift to lower track densities for the recently measured distribution. We do not yet understand the reason for this. It has nothing to do with the image analysis techniques. The problem probably arises from one of two sources: a

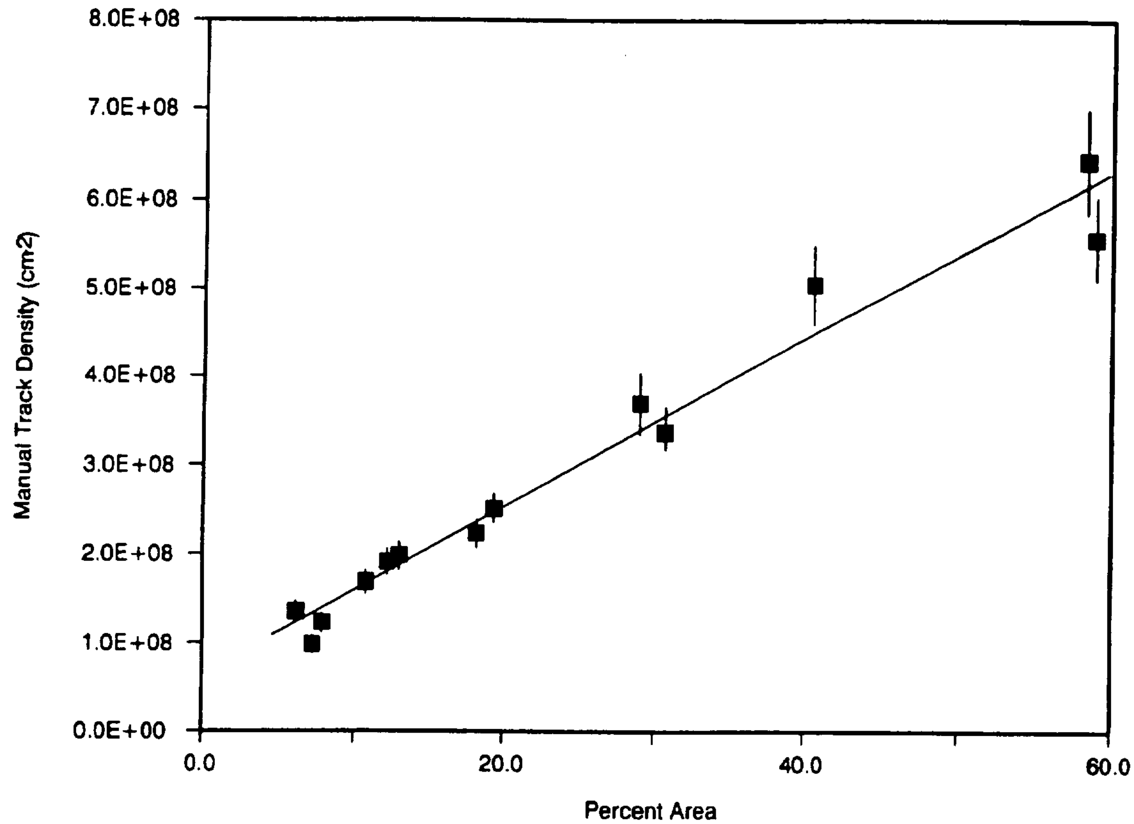

Figure 4. Track densities counted manually versus the percent area of the image covered by tracks. These quantities correlate with a coefficient r=0.98. The line is the linear regression line which best fits the points.

systematic error in magnification for one data set or the other, or a bias against high density grains in this work knowing that they could not be counted using these techniques. It should be noted that the highest density column in the first histogram consists of grains that were deemed uncountable by the observers.

CONCLUSIONS

This summer project has shown that we can measure track densities in lunar grains using image analysis techniques. It is difficult to assess exactly how much more time efficient this method will be. During the course of the study we used 191 digital images most of which have been saved on floppy disks (this procedure is surprisingly slow for this computer). We had ~14 sessions (~6 h each)of microscope time, but it was the last two sessions that we used more or less in the "production" mode of generating scientific data rather than testing and adjusting the procedures. Even during these sessions, however, we keystroked the procedures rather than use macros to speed up the process. In the application

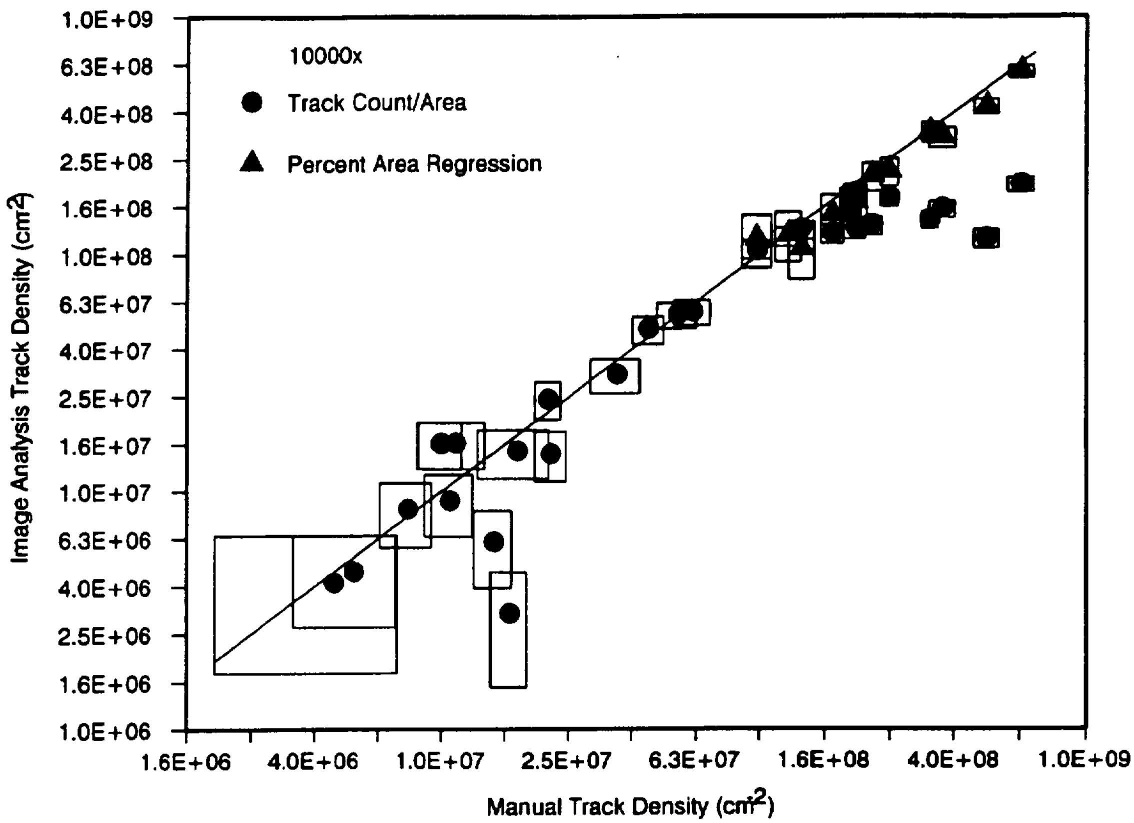

Figure 5. The correlation of manually counted and image analysis determined track densities for data taken at 10000x. Circles represent data obtained using feature scan and triangles represent data using a linear regression formula of the percent area. Rectangles give one standard deviation uncertainty based on counts or the error in the regression formula.

we chose to demonstrate we measured a more detailed distribution than had been reported in the past. An equally valid task would have been to measure distributions at more different depths in the core (the original study measured distributions 12 mm apart except in critical regions (Blanford *et al.*, 1979)). Either task requires making individual measurements on grains at a faster rate which we have shown can be done.

Track morphological characteristics are related to the energy loss rate of the ionizing particle that made the track. Plastics are used as cosmic ray dosimeters by measuring the density and energy loss of ionizing radiation from the tracks it produces (Price and Fleischer, 1971; Fleischer *et al.*, 1975). These measurements are also possible using image analysis techniques and represent a possible future direction of these studies.

REFERENCES

Blanford G.E., Blanford J., and Hawkins J.A. (1979) Irradiation stratigraphy and depositional history of the Apollo 16 double drive tube 60009/10. *Proc. Lunar and Planetary Sci. Conf. 10th*, 1333-1349.

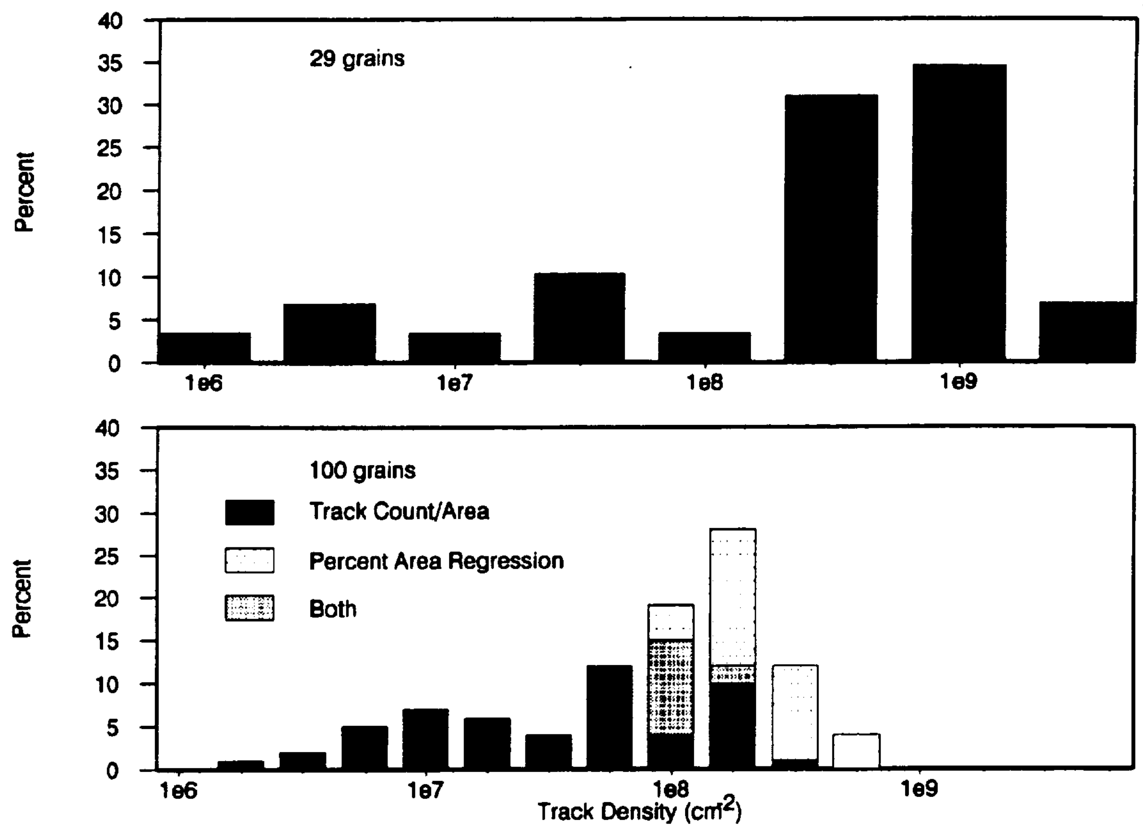

Figure 6. Histograms of the track density distribution at 546 mm below the lunar surface in sample 60009,6049. The upper histogram is based on manual measurements in 29 grains made 15 years ago. The lower histogram is based on 100 grains using image analysis techniques this summer. The bimodal distribution clearly indicates that this soil consists of a mixture of two components with different exposure histories. The distribution based on a larger number of grains is much easier to interpret.

Fleischer R.L., Price P.B., and Walker R.M. (1975) *Nuclear Tracks in Solids: Principles and Applications.* University of California Press, Berkeley, CA.

McKay D.S., Heiken G., Basu A., Blanford G., Simon S., Reedy R., French B.M., and Papike J. (1991) The lunar regolith. In *Lunar Sourcebook: A User's Guide to the Moon* (G. Heiken, D. Vaniman, and B.M. French, ed.), pp. 285-356. (Cambridge University Press, Cambridge).

Price P.B. and Fleischer R.L. (1971) Identification of energetic heavy nuclei with solid dielectric track detectors: Applications to astrophysical and planetary studies. *Ann. Rev. Nuc. Sci.* **21**, 295-334.

Price P.B. and Walker R.M. (1962) Electron microscope observation of etched tracks from spallation recoils in mica. *Phys. Rev. Letters* **8**, 217-219.